Perspective

Charge-neutral electronic excitations in quantum insulators

https://doi.org/10.1038/s41586-024-08091-8

Received: 29 March 2021

Accepted: 20 September 2024

Published online: 13 November 2024

Check for updates

Sanfeng Wu[1]✉, Leslie M. Schoop[2], Inti Sodemann[3], Roderich Moessner[4], Robert J. Cava[2] & N. P. Ong[1]✉

Experiments on quantum materials have uncovered many interesting quantum phases ranging from superconductivity to a variety of topological quantum matter including the recently observed fractional quantum anomalous Hall insulators. The findings have come in parallel with the development of approaches to probe the rich excitations inherent in such systems. In contrast to observing electrically charged excitations, the detection of charge-neutral electronic excitations in condensed matter remains difficult, although they are essential to understanding a large class of strongly correlated phases. Low-energy neutral excitations are especially important in characterizing unconventional phases featuring electron fractionalization, such as quantum spin liquids, spin ices and insulators with neutral Fermi surfaces. In this Perspective, we discuss searches for neutral fermionic, bosonic or anyonic excitations in unconventional insulators, highlighting theoretical and experimental progress in probing excitonic insulators, new quantum spin liquid candidates and emergent correlated insulators based on two-dimensional layered crystals and moiré materials. We outline the promises and challenges in probing and using quantum insulators, and discuss exciting new opportunities for future advancements offered by ideas rooted in next-generation quantum materials, devices and experimental schemes.

In crystalline solids, electrons are packed closely together and interact strongly by means of the Coulomb force. In the standard Landau model, the electronic quasiparticle excitations are viewed as dressed weakly interacting fermions although they couple to external electric and magnetic fields by means of their electric charge. This powerful description—valid in familiar metals, semiconductors and insulators—has worked well in condensed matter physics. It underlies virtually all modern electronics-based technologies from transistors, solar cells and light emitting diodes to superconducting devices.

However, materials that do not obey this conventional description do exist. An example is the situation of interacting electrons confined to a one-dimensional (1D) wire, in which the Luttinger liquid theory, rather than Landau's Fermi liquid theory, serves as the standard description[1]. The low-energy excitations in a Luttinger liquid are fractionalized modes that separately carry spin and charge degrees of freedom. In two-dimensional (2D) and three-dimensional (3D) systems, non-Fermi liquid physics has increasingly occupied centre stage in research on strongly correlated materials, including cuprates[2], heavy fermion materials[3,4] and, more recently, moiré materials[5–8]. Beyond non-Fermi liquids, strongly correlated electrical insulators may also show striking properties that go beyond the conventional picture. This is the theme of our Perspective. We review how the conventional quantum theory of solids may break down in electrical insulators, discuss the current experimental status and outline promising future directions. We focus on insulators showing interesting charge-neutral electronic excitations in the bulk that cannot be captured by conventional band theory.

Theoretical overview of neutral excitations

Up until the 1970s it was widely believed that excitations in many-electron systems would always carry an integer multiple of the electron charge, and that particles with an even (odd) multiple of electron charge would necessarily be bosons (fermions). Charge-neutral excitations such as excitons (bound electron-hole pairs) or magnons (spin excitations in a magnet) were expected to be bosons. The discoveries of fractionalization in 1D polymer chains[9,10] and the fractional quantum Hall (FQH) effect in 2D electron gases[11] disrupted this morel by demonstrating that materials can harbour quasiparticles with a fractional electron charge (Fig. 1a). Moreover, quasiparticles in fractionalized electronic systems can have anyonic exchange statistics[12–14] and are therefore fundamentally different from bosons or fermions.

Separately, Anderson proposed his seminal ideas of the resonant valence bond (RVB) 'spin liquid' states[15], which gained much prominence as proposed parent states of high-temperature superconductors[16]. The RVB proposal led to strong debate. A model showing a bona fide RVB spin liquid phase was found a few decades later[17]. The RVB spin liquid and the FQH states are now understood to be examples of a large class of fractionalized states[18]. For example, the short-range RVB liquid in the absence of symmetry represents the same topological phase[18] as the toric code introduced by Kitaev[19]. These are often referred to as Z_2 spin liquids on account of the local Ising (Z_2) symmetry of the emergent gauge field.

[1]Department of Physics, Princeton University, Princeton, NJ, USA. [2]Department of Chemistry, Princeton University, Princeton, NJ, USA. [3]Institute for Theoretical Physics, University of Leipzig, Leipzig, Germany. [4]Max-Planck Institute for the Physics of Complex Systems, Dresden, Germany. ✉e-mail: sanfengw@princeton.edu; npo@princeton.edu

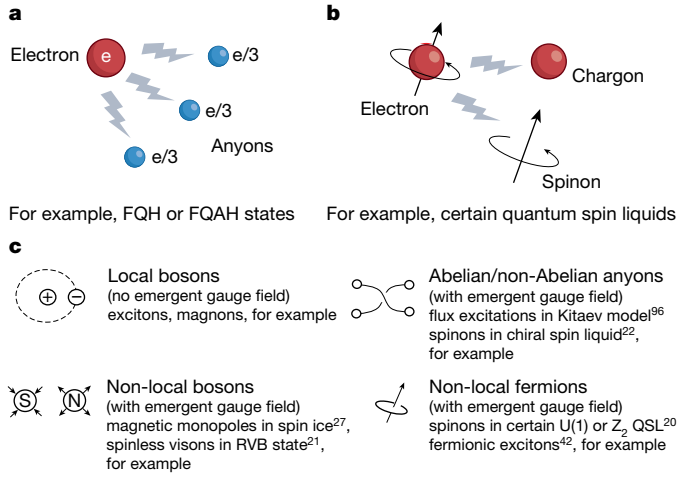

Fig. 1 | Electron fractionalization and charge-neutral excitations in quantum insulators. a, Cartoon illustration of charge fractionalization in the FQH effects. FQAH, fractional quantum anomalous Hall. **b**, Cartoon illustration of spin-charge separation in QSL arising in, for example, correlated Mott insulators. **c**, A selection of charge-neutral excitations in electrical insulators with possible model realizations, with selected references listed.

Indeed, the presence of emergent deconfined gauge fields is often considered to be the defining feature of a spin liquid. The emergent gauge field in spin liquids comes with accompanying particles that are charged under it. The deconfinement is the property that these particles can be separated arbitrarily far away from each other with a finite energy cost. This endows them with a non-local aspect: they are sources or sinks of a corresponding emergent flux, just as an electron is a source of electric field on account of its electric charge. These particles, neutral with respect to Maxwell electromagnetism, can have different quantum statistics: fermionic, bosonic or anyonic. There certainly is no need for all neutral particles to be bosons. They can carry quantum numbers that are fractions of those of the microscopic degrees of freedom[20–22]. For example, in an RVB liquid, adding an electron can generate two independent particles: a spinon that carries the spin and a chargon that carries the electric charge (Fig. 1b).

Mathematically, the case of an emergent U(1) gauge field is very close to Maxwell electromagnetism, which is also a U(1) gauge theory. However, details can differ greatly: the emergent theory can harbour both electric and magnetic emergent charges, and show a much larger fine-structure constant[23]. One can even study the emergent analogue of Maxwell theory in two dimensions. However, this is believed to be stable only when the gauge field coexists with gapless fermionic degrees of freedom charged under this gauge field[24,25]. These fermions could be nodal (as in, for example, Dirac spin liquids) or have a Fermi surface (as in, for example, the 'spinon Fermi surface state'). In three dimensions, the U(1) gauge structure can remain stable even in the absence of gapless fermionic degrees of freedom. A model system known as spin ice, a paradigmatic model showing an emergent U(1) 3D gauge structure (refs. 26,27), features emergent electric and magnetic charges[28]. Figure 1c summarizes properties and occurrences of selected charge-neutral quasiparticles in insulators.

The electromagnetic response of correlated insulators with fractionalized excitations is rich and complex. Local probe fields can only create multiplets of fractionalized quasiparticles, as the net quantum numbers of the product of a scattering process cannot be fractional. Unlike the case of neutrons scattering off single magnons, it is therefore generally not possible to obtain a sharp response even from long-lived fractionalized quasiparticles. The coupling matrix elements can further differ hugely from those of conventional electromagnetism, not least on account of different symmetry properties of emergent fields; for instance, emergent magnetic fields can be even under time reversal. Nonetheless, U(1) spin liquids with gapless fermions can in principle show striking experimental consequences, including subgap power law optical conductivity[29], quantum oscillations in response to magnetic fields[30,31], cyclotron resonance in the absence of charged quasiparticles[32] and metallic-like magnetic noise[33] and so on. All these provide new avenues for their experimental detection. See more discussions and their implications on measurable quantities in Box 1.

Experimental progress, challenges and opportunities

Experimentally, the detection of quantum properties of insulators and charge-neutral excitations is hampered by the lack of suitable low-temperature probes. Thermal transport is one of the few techniques available for investigating excitations in insulators at low T in strong magnetic fields. Whereas it is a powerful probe for 3D materials, it faces challenges in 2D materials, a growing platform for many interesting insulating phases. Other conventional approaches, such as electrical transport and tunnelling spectroscopy, are not directly sensitive to charge-neutral excitations, especially when the charge gap is large. This limitation may explain why experimental progress in 2D insulators has been slow except in insulators with a gap less than roughly 100 meV. Next, we discuss the status and perspective for the experimental detection of hidden quantum phenomena in insulators, focusing on selected topics in both 3D bulk materials and the rapidly evolving correlated 2D crystals and van der Waals (vdW) stacks.

Excitonic insulators

The first prominent case we highlight is the excitonic insulator. In the single-particle band picture, we have a band insulator if a fully occupied valence band is separated from the conduction band by a finite energy gap E_g. This picture is modified when the gap is small because Coulomb interaction leads to bound states (excitons) of electrons in the conduction band and holes in the valence band[34–36], as sketched in Fig. 2a. This effect occurs when the exciton binding energy E_{ex} exceeds the band gap E_g. A similar situation is obtained in low carrier-density semimetals in the limit of weak screening of the Coulomb interaction. The formation of excitons converts the semimetal to an insulator, as pointed out by Mott[37]. Theories of excitonic anomalies near the semimetal-semiconductor transition are reviewed in detail in ref. 38.

In brief, in weakly interacting band insulators there is an energy gap to create excitons. However, as the electron repulsions increase this gap can decrease leading to quantum phase transitions into a new state in which excitons spontaneously 'proliferate', without a closing of the charge gap. When the exciton is an ordinary local boson (Fig. 1c) the resulting state would be an insulator with a spontaneously broken symmetry[38]. In this case, the excitonic insulator can represent a special subset of broken symmetry states in which the exciton condensation is also accompanied by some robust form of nearly gapless fluidity of neutral modes, which remains robust throughout the phase of matter itself and not just near a critical point. One mechanism for this is that the exciton carries a quantum number associated with a continuous symmetry, then its condensation leads to the existence of broken symmetry (quasi-) Goldstone modes. Another mechanism is that the exciton carries a momentum that is incommensurate with the reciprocal Bravais vectors, and the broken symmetry state resulting from the exciton condensation will be an incommensurate charge density wave, spin density wave[38] or spin spiral state[39,40], whose sliding modes will remain partly soft and cannot be completely pinned by the atomic crystal. There can also be more exotic forms of exciton proliferation[41,42], which are not necessarily local bosons and can lead to protected gapless fluid neutral modes, such as the composite exciton fermion[42] (Fig. 1c).

Experimental confirmation of an excitonic insulator in crystals is challenging because the excitons are intrinsic to the ground state and are charge-neutral. Note that exciton physics in optically excited

Box 1

Fractionalization and emergent gauge fields in insulators

An exactly soluble model

Kitaev's honeycomb model[96] is exactly soluble and may also be relevant for experiments on candidate materials. Its Hamiltonian (H_K), in the simplest incarnation, reads

$$H_K = \sum_{ij,\alpha} \sigma_i^\alpha \sigma_j^\alpha,$$

where the sum is over all nearest neighbour pairs ij. It is 'spin-orbit coupled' in that the spins only interact by means of one component of their spin (given by Pauli matrix σ^α, $\alpha = x, y, z$) depending on the bond direction, as depicted in Fig. 3d.

An elegant way to demonstrate fractionalization is to directly identify the degrees of freedom carrying the fractional quantum numbers. We write the spin-1/2 operators as a combination of four Majorana operators, three 'bond Majoranas' b_i^α and one 'matter Majorana' c_i. Majorana operators have commutation relations $\{b_i, b_j\} = 2\delta_{ij}$ and are often referred to as 'real fermions', as a pair of them can be combined to a standard complex fermion, f, as $f^\dagger = (c_1 - ic_2)/2$. The model has a set of non-dynamical (that is, conserved and immobile) flux operators, $W_p = \prod \sigma_i^\gamma$, one for each hexagon plaquette p of the honeycomb lattice. Here, the product defining W_p runs over the six sites of p, with γ the bond direction pointing out of the hexagon at site i. On writing $S_i^\alpha = b_i^\alpha c_i$, one obtains that the W_p operators are entirely made from the 'bond Majoranas' b_i^α. The values of all W_p can independently take ±1 (that is, they are Z_2 degrees of freedom), and together they define a flux sector. The Kitaev honeycomb model can then be exactly solved, flux sector by flux sector, by considering a fermionic hopping problem for the matter fermions (f and $f^\dagger$) subject to the background fluxes W_p.

Fractional excitations

This solubility illustrates explicitly several general features of fractionalization: the microscopic spin degrees of freedom have been replaced by more 'natural' emergent variables, the matter fermions and fluxes. These emergent variables capture the 'breaking apart' of the spin degrees of freedom. In principle, one obtains such a form of the Hamiltonian from more general parton constructions, whose use depends on how naturally the chosen construction reflects the actual low-energy degrees of freedom of the many-body problem under consideration. When the itinerant fermions (f and $f^\dagger$) have a gapped spectrum with Chern number ±1, the Kitaev model realizes a non-Abelian fractionalized state. There are two kinds of quasiparticles in the bulk of this non-abelian state: the complex itinerant fermions (f and $f^\dagger$) and the Ising flux-like particle (the vison) associated with the above plaquette operator. A vison is present (absent) in a plaquette when $W_p = -1$ ($W_p = +1$). The vison particle, which is an analogue of an Abrikosov vortex in a superconductor, carries a Majorana zero mode in its core and shows non-Abelian exchange statistics. Figure 1c summarizes neutral excitations in selected models.

Responses

How does a physical electromagnetic field couple to the emergent degrees of freedom? The answer in general is clear: it depends. On the level of the microscopic Hamiltonian, a simple Zeeman field h^α in the Kitaev model couples to both matter fermions and fluxes: $h^\alpha S_i^\alpha = i\, h^\alpha b_i^\alpha c_i$. Its action on the fractionalized system can hence be involved: for example, it can give dynamics to the flux degrees of freedom, while also changing the matter degrees of freedom. This illustrates why the coupling to electromagnetic fields is so diverse in fractionalized systems; simple-looking couplings turn out to be complex once the spins have broken apart.

Indeed, each fractionalized model in principle comes with its own coupling to external fields, which will depend on symmetry properties of the emergent degrees of freedom as well as underlying microscopic details. For example, in the case of U(1) quantum spin liquid (QSL) featuring a spinon Fermi surface, Landau quantization may develop as a response of the spinon-gauge field system to an external magnetic field[30]. In quantum spin ice, fractionalization leads to an emergent gauge field that has photons, electric charges (spinons) but also—unlike the world we inhabit—magnetic charges (Fig. 1c). How an externally applied electromagnetic field couples to these depends on microscopic features, such as: do the spins derive from ions with an even or an odd number of electrons? In the latter case, time-reversal symmetry, as expressed, for example, in Kramers theorem, forbids certain couplings of an electric field to the fractionalized excitations.

Generally, the Hamiltonian of the fractionalized particles involves not only the emergent gauge coupling, but also 'remembers' properties such as the crystal field scheme of the microscopic spins. Determining many features in detail is a challenge for each material individually. Nonetheless, simple behaviour can emerge from qualitative considerations. In the case of spin ice, the fractionalized quasiparticles are sources of both an emergent field as well as the usual (Maxwell) magnetic field—hence their appellation as magnetic monopoles. Such a combination has been termed a hybrid dyon[178], and it can lead to effects, superficially familiar from metallic systems, appearing in new ways in insulators. An interesting prediction is a magnetic Nernst effect in insulators, in which applying an electric field perpendicular to a temperature gradient induces a magnetization perpendicular to both[178].

semiconductors is well established and has been extensively studied in the past decades in 2D semiconducting transition metal dichalcogenides[43,44]. One can straightforwardly observe signatures of optical excitons in photoluminescence measurements as these excitons can decay by emitting light. In excitonic insulators, excitons are the lowest energy state and their observation is not straightforward.

Experimental investigation of excitonic insulators fall into two categories: (1) artificial electron-hole bilayers, in which investigation of exciton condensates has been systematically conducted in quantum Hall bilayers consisting of two closely spaced 2D electron gases placed in high magnetic fields[45–47]. Striking consequences of the quantum Hall exciton condensate include Josephson-like quantum tunnelling, Coulomb drag and counterflow transport and so on, as observed in both semiconductor quantum wells and graphene[45–47]. Evidence for an excitonic insulator state in zero magnetic field has also been reported in InAs/GaSb bilayers[48,49] and more recently in several vdW bilayers or trilayers of transition metal dichalcogenides[50–52] (Fig. 2b). (2) Natural crystals. Whereas the excitonic insulator theory was originally developed for bulk crystals, its experimental detection has been more challenging. Candidate bulk crystals include 1T-$TiSe_2$ (refs. 53–55), Sb nanoflakes[56], Ta_2NiSe_5 (refs. 57–61) and recently $Ta_2Pd_3Te_5$ (refs. 62,63) (Fig. 2b). A common challenge in identifying

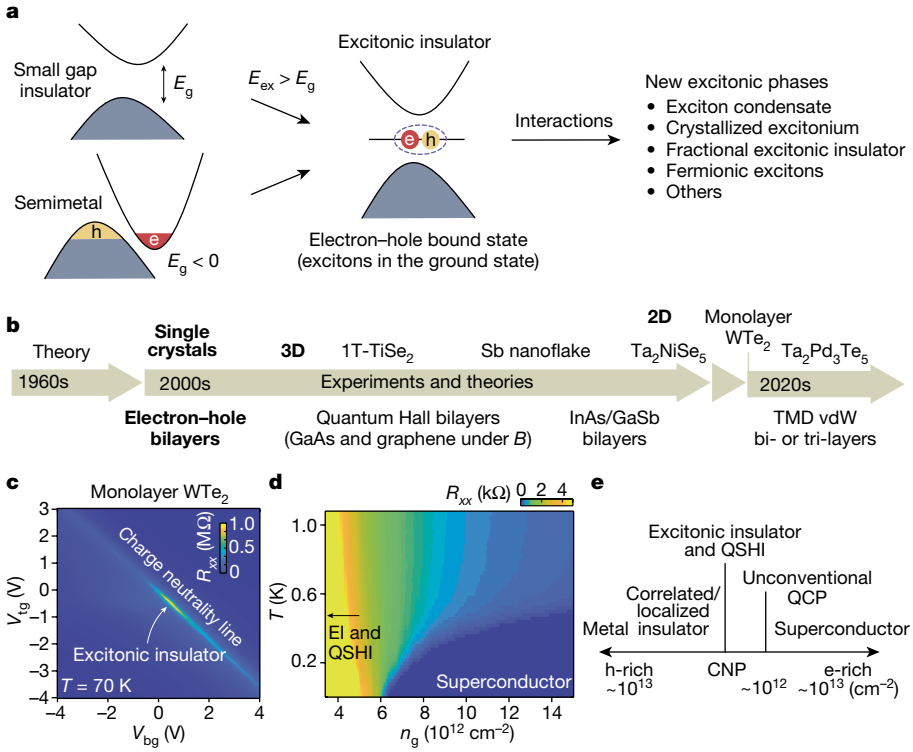

Fig. 2 | Excitonic insulators. a, Sketches of the formation of excitons in small gap insulators or semimetals in a band picture. **b**, Selected excitonic insulator materials investigated so far. **c**, Resistance map of monolayer WTe_2 as a function of top (V_{tg}) and bottom (V_{bg}) gate voltages. The insulator state that appears at the charge neutrality line is the topological excitonic insulator state. Plot reproduced from ref. 64. **d**, A resistance phase diagram of monolayer WTe_2 on electron doping, in which a superconducting state is developed next to the excitonic insulator. **e**, A sketch of the phase diagram of monolayer WTe_2 covering both electron- and hole-doped regimes.

an excitonic insulator phase in bulk crystals is to distinguish it from a trivial band insulator especially because structural transformations in these systems generate ongoing debates (for example, ref. 61). In 2021, a 2D crystal, that is, monolayer WTe_2, was identified as an excitonic insulator [64,65]. Figure 2c plots the resistance of monolayer WTe_2 as a function of the top and bottom gate voltages typically used for 2D devices, highlighting the appearance of the excitonic insulator state at charge neutrality. The gate tunability of a 2D crystal allows for new opportunities in characterizing an excitonic insulator. In particular, the gate-tuned tunnelling spectra[64] of monolayer WTe_2 show that the insulator phase originates from electron correlations and rule out the possibility of a band insulator. This key conclusion is further supported by gate-tuned measurements of the chemical potential[65] and an anomaly in the gate-tuned Hall effect[64]. Such gate-tuned measurements are infeasible in bulk crystals.

Therefore, 2D WTe_2 serves as an exciting test bed for investigating characteristics of excitonic insulators[39,40,64–66]. The promise is further highlighted by the many other properties of this material, including (1) the excitonic insulator is also a quantum spin Hall insulator (QSHI)[67–70], (2) a superconducting phase emerge when a moderate density of electrons is introduced to the excitonic insulator[71,72] (Fig. 2d), (3) a distinct intriguing phase[64,65,68,70,73] on the hole-doped side (Fig. 2e) and (4) unexpected Landau quantization that appears in the insulating regime[73,74] (discussions in the section 'Case III: the search for charge-neutral Fermi surfaces in insulators' below). Moreover, the recent finding of an unconventional quantum critical point[75] located in between the excitonic insulator phase and the superconducting phase highlights a deeper connection between the two to be discovered. The topological excitonic insulator state at charge neutrality, as the pristine property of the monolayer, is core to unlock the many intriguing mysteries associated with the rich low-T phenomena in this material.

The field of excitonic insulator has gained new impetus and more excitonic insulator materials are emerging. In general, interactions in the many-exciton state of an excitonic insulator are likely to generate a diverse variety of phases. The main challenge is that our experimental approaches for investigating a charge-neutral state are immature such that examinations of even the plain vanilla version of an excitonic insulator remain difficult.

QSLs

The QSL state was proposed by Anderson in 1973 (ref. 15) as a new kind of insulator that shows a liquid-like ground state of spins on a lattice with geometric frustration (Fig. 3a). Subsequent theoretical work has shown that the QSL may host exotic fractional excitations and the emergent gauge fields. One remarkable possibility is that there is a class of gapless QSL featuring a spinon Fermi surface accompanied with an emergent U(1) gauge field. Although it is true that the spinons do not carry charge under the physical magnetic field, the internal gauge field may couple to the external magnetic fields. For instance, the emergent U(1) gauge field structure may allow for the appearance of an emergent magnetic field whose average value itself can be induced by an external magnetic field in some situations[30,31,76], producing spinon Landau quantization. Several recent reviews on QSLs summarize both the theoretical and experimental advances so far[77–81]. Despite much progress, however, the existence of a QSL state in a physical material remains an open question.

We first highlight the experimental challenges on this topic by tracing the studies of one specific QSL candidate 1T-TaS_2, a vdW layered material named in Anderson's original paper[15]. This material was not widely recognized as a QSL candidate until 2017, when Law and Lee provided arguments[82] empowered by modern views. A possible spinon Fermi surface state in 1T-TaS_2 was later proposed[83]. At low T, the material develops an insulating charge density wave consisting of clusters of stars of

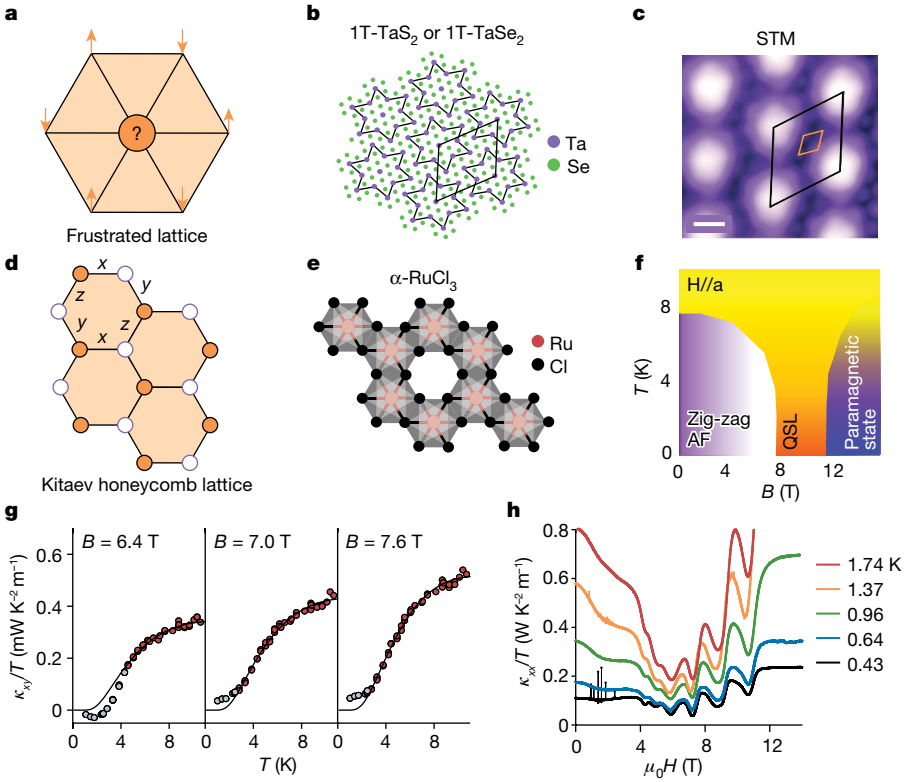

Fig. 3 | QSLs. a, An illustration of geometric frustrations of spins on a triangular lattice. **b**, The lattice of QSL candidate 1T-TaS_2 and 1T-$TaSe_2$, showing clusters of stars of David that form a triangular superlattice. Plot reproduced from ref. 89. **c**, A scanning tunnelling microscope image of 1T-$TaSe_2$, showing the superlattice. Plot reproduced from ref. 89. Scale bar, 5 Å. **d**, The honeycomb lattice of the Kitaev model. **e**, The crystal structure of α-$RuCl_3$. Plot reproduced from ref. 98. **f**, A sketch of the phase diagram of α-$RuCl_3$. Plot reproduced from ref. 110. **g**, Thermal Hall response, κ_{xy}/T, as a function of T measured in α-$RuCl_3$, at selected values of magnetic field B. The solid lines are fits to the data. Plot reproduced from ref. 109. **h**, Thermal conductivity response of α-$RuCl_3$, κ_{xx}/T, as a function of magnetic field, taken at selected values of T. Plot reproduced from ref. 110.

David, forming a triangular superlattice (Fig. 3b). Experimental studies on the nature of this state, in principle a Mott insulator, are challenging. Investigations of its bulk form involves the interlayer stacking order, which complicates the situation[84–88]. Studies on monolayer 1T-TaS_2, a much stronger insulator compared to its bulk, can clear out the situation but little is known about the monolayer. Recently, scanning tunnelling microscope studies of monolayer 1T-$TaSe_2$ (a sister material of 1T-TaS_2) grown on metallic graphene substrates (Fig. 3c), necessary for charge transport, have shown interesting results consistent with the Mottness and possible QSL state[89–91]. However, the low-T properties of the pristine monolayers of 1T-TaS_2 or 1T-$TaSe_2$, either isolated or on an insulating substrate, remains unknown due to the lack of proper experimental tools to diagnose such a strong 2D insulator. Similar studies and status can be found in the isostructural 1T-$NbSe_2$ (refs. 92–95).

Another topical area of QSL research is the search for materials that are proximate to the Kitaev honeycomb model Hamiltonian[96] H_K that describes spin-1/2 Ising spins interacting with bond-specific exchange couplings (Box 1 and Fig. 3d)[80,96,97]. Following calculations[97] pointing to the 4*d* and 5*f* chalcogenides as likely platforms, α-$RuCl_3$ (Fig. 3e) was identified as the closest proximate[98]. The Ru ions, which carry a spin-1/2 moment, occupy the sites of the honeycomb lattice. In zero magnetic field, α-$RuCl_3$ orders at 7 K as an antiferromagnet (with zig-zag order stabilized by terms not included in H_K). An in-plane field **H**, applied parallel to the zig-zag axis **a**, causes long-range order to vanish sharply at a critical field B_{c2} = 7.3 T. As H increases above roughly 10 T, sharp magnon modes emerge in the spectrum. The interesting state in between (7.3 T < H < 10 T), characterized by a broad, featureless spectrum of excitations, has been widely discussed as a QSL state relatable to H_K (refs. 98–106) (Fig. 3f). Both the spin liquid and zig-zag states have been investigated by neutron scattering[98], electron spin resonance[107], terahertz spectroscopy[108], thermal transport[109,110] and so on.

Interest spiked following a report that, within a narrow temperature window (3.7 and 4.9 K), the thermal Hall conductivity κ_{xy} in the QSL interval seemed to show[111] a half-quantized value in accord with Kitaev's calculation, both with **H** tilted out of plane[111] and with **H**||**a** (the zig-zag axis)[112]. In this scenario, the heat current is carried by Majorana excitations that occupy chiral edge modes. However, subsequent experiments have not validated the finding of half-quantization. Measurements extended to a much broader interval in T (0.5 to 10 K, with **H**||**a**) show[109] that κ_{xy} arises from excitations that obey the Bose–Einstein distribution. In the proposed picture, the spin excitations occupy a topological band, and are subject to a large Berry curvature that changes sign with **H**||**a** (ref. 113). Fits to the Murakami expression for κ_{xy} yield a Chern number (of the lowest spin band) close to 1 above 9 T (Fig. 3g). Moreover, the inferred band energy is roughly 1 meV, in good agreement with previous microwave absorption and electron spin resonance experiments. Subsequent experiments comparing crystals grown under different conditions again do not observe half-quantization. There is one report[114] that argues that κ_{xy} may approach the half-quantized value for H larger than 10 T. In this regime, however, the uncertainties in κ_{xy} diverge uncontrollably because the thermal Hall resistivity λ_{yx} rapidly vanishes[109].

Another finding in α-$RuCl_3$ is that, below 4 K, the thermal conductivity κ_{xx} shows large oscillations versus H (with **H**||**a**)[110] (Fig. 3h). Although α-$RuCl_3$ is an excellent charge insulator, the κ_{xx} curves resemble Shubnikov–de Haas oscillations in a semimetal. The integers n indexing the extrema in κ_{xx} vary linearly with 1/H, except for a sharp break in slope near B_{c2} = 7.3 T. The oscillation amplitudes are strongly enhanced within

the QSL field interval (7.3, 10) T although a tail of attenuated oscillations persists to 4 T, deep in the zig-zag state. In the four samples studied[110], the oscillations are closely similar both in phase and period, but the amplitudes are sample dependent. An interesting interpretation is that, despite the complete absence of free electrons, long-lived neutral fermionic excitations seem to define an effective Fermi surface. These fermions have been proposed to be pseudo-scalar spinons[115] to reconcile the presence of oscillations of κ_{xx} concomitant with absence of κ_{xy} when the in-plane field is along **b** (the armchair axis). Note that Landau quantization is not expected for the original Kitaev model. Alternately, the oscillations are modulations of the dominant phonon conductance caused by periodic oscillations of the spin density of states that modulate the scattering amplitude between phonons and spin excitations.

Subsequently, oscillations in κ_{xx} versus H were observed by Bruin et al.[116] in crystals of α-$RuCl_3$ showing a large spread of T_Ns from 7 to 13–14 K, which they attributed to a cascade of stacking faults. Originally, Kubota et al.[117] had proposed that sweeping H at $T < 4$ K induces several transitions caused by stacking-fault creation. Kubota et al. linked several features in the field profile of the magnetic susceptibility at 4 K to the large spread of T_N by angular extrapolation within the *T*-*H* plane. Later, Cao et al.[118] showed that the spread in T_Ns (especially the 14 K transition in the magnetization) in a given crystal provides a reliable signature of high stacking-fault density (this test is now widely adopted to screen crystals with high stacking-fault density). Bruin et al.[116] adopted Kubota's cascading scenario to identify the oscillations with successive transitions by field-creation of stacking faults at low T (also ref. 119). Zhang et al.[120,121] have tested this association by monitoring the oscillations in a series of crystals in which the stacking-fault density is controlled. They found that the oscillation period is actually closely similar in all crystals irrespective of stacking-fault density, with amplitude largest in crystals with lowest stacking-fault density. They conclude that the oscillations are unrelated to the 14 K transition. We note that none of the crystals used in ref. 110 shows the 14 K transition or even a spread of T_Ns. Together, these studies strongly disfavour the cascading transition scenario. We further remark that the stochastic nature of field-induced stacking fault should lead to widely different oscillation periods (and hysteresis) in conflict with all reports to date. A recent experiment[122] on the dependence of the thermal conductivity versus the azimuthal angle of the in-plane **H** reveals an angular variation consistent with an intrinsic property of the QSL state. Future experiments examining other quantities beyond thermal conductivity may provide new insights into the nature of this intriguing state. More recently, Hong et al.[123] reported κ_{xx} versus H measured in the Kitaev material $Na_2Co_2TeO_6$, which shows two prominent dips at low T for both field orientations (**H** along armchair or zig-zag axes). Hong et al.[123] propose that these features, which roughly resemble the oscillations reported by Czajka et al. in α-$RuCl_3$, arise from phonon scattering from magnetic structures or domains in the spin-disordered state in $Na_2Co_2TeO_6$.

The search for charge-neutral Fermi surfaces in insulators

The quest to find insulators that show a neutral Fermi surface (for example, QSL with a spinon Fermi surface) has long been a challenge in condensed matter physics. Unlike in conventional insulators, the thermal conductivity here is predicted to show a metallic temperature profile at very low temperatures. This is one of the key tests[77–79] so far adopted in many experiments, for example, on organic materials[77] and 3D quantum magnets[124]. At present, there is considerable debate on the results and their interpretations (for example, refs. 125–127). A central feature of the spinon Fermi surface is the emergent gauge field that couples to spinons in a way similar to the coupling of the electromagnetic fields to electrons. This leads to observable effects if the emergent gauge field further couples to electromagnetic fields.

A useful concept governing the electromagnetic response of a fractionalized system is the Ioffe–Larkin rule[128,129]. For example, electronic transport in a spin-charge separated material involves both spinon transport and chargon transport. However, the source and drain metal electrodes can only inject/accept electrons, which fractionalize into spinons and chargons within the material. By the Ioffe–Larkin rule, the measured resistivity (not conductivity) is the sum of the spinon resistivity and chargon resistivity. An intriguing case is the Landau quantization of the spinon Fermi surface in magnetic fields[30], which can in principle lead to quantum oscillations of observables in insulators[30,31,130]. Experimentally, the quantum oscillations look similar to the Shubnikov–de Haas and de Haas–van Alphen effects in metals.

Although quantum oscillations in insulators have been reported in several systems including Kondo insulators SmB_6 (refs. 131,132) and YbB_{12} (ref. 133), quantum wells[134,135], topological excitonic insulator WTe_2 (ref. 73), the QSL candidate α-$RuCl_3$ (ref. 110) and more recently on YCu_3-Br (ref. 136), the discussion of their interpretations remains widely open[116,119,122,137–149]. In the previous section, we summarized the status of oscillations observed in α-$RuCl_3$. A conclusive demonstration of a neutral Fermi surface inside a charge gap remains an outstanding goal. It is essential to establish a concrete case in which intrinsic Landau quantization in insulators can be firmly established experimentally. This requires a combination of techniques for detecting quantum oscillations that simultaneously excludes competing explanations.

We highlight the promise of achieving such a goal in monolayer WTe_2 and subsequently strongly correlated 2D materials systems. Quantum oscillations in monolayer WTe_2 insulators were first reported in the resistance measurements[73]. The most striking observation lies in the apparent conflict between the measured low conductivity (σ) of the resistive state (greater than 100 MΩ) and the high carrier density ($n > 10^{12}$ cm^{-2}) with high mobility ($\mu > 1{,}000$ cm^2 V^{-1} s^{-1}) extracted from the quantum oscillation data[73]. In other words, $\sigma \ll ne\mu$. A natural interpretation to resolve this conflict is to assign the highly mobile carriers responsible for the quantum oscillations to be charge neutral. This is the neutral fermion picture. In alternative explanations, these highly mobile particles are ordinary charge carriers, either thermally activated or residing in the metal component used in the device. In one scenario (1), they are charge carriers thermally activated across the gap, and the quantum oscillations of the insulator are interpreted as the consequence of the B-induced oscillations of the insulator gap[66,144]. In a second scenario (2), the highly mobile carriers reside in the nearby graphite gate, whereas carriers in monolayer WTe_2 merely serve to detect Landau levels in graphite[145].

To distinguish these scenarios, one needs to go beyond electrical transport measurements. In particular, measurements of quantum oscillations in the thermoelectric response of monolayer WTe_2 have considerably clarified the situation[74,150]. Distinct from the conductivity, the Seebeck effect is sensitive to the derivative of the density of states with respect to energy and hence to the energy structure near the chemical potential. For instance, in a Landau quantized 2D electron gas, the Seebeck signal will develop a sign-change oscillation each time when the Fermi level is crossed by a Landau level (for example, observations in graphene[151,152]), signifying that the carrier type has altered its character effectively from 'hole-like' to 'electron-like' (Fig. 4a,b). Such sign-change thermoelectric quantum oscillations have been observed recently in the WTe_2 monolayer insulator in the hole-doped regime[74] (Fig. 4c–f), indicating that the highly mobile carriers responsible for the quantum oscillations belong to WTe_2 insulator itself and that a Landau level-like energy structure is developed in magnetic fields near the chemical potential. The alternative scenarios (1) and (2) are not supported by the thermoelectric data. In the neutral Fermi surface scenario, the Ioffe–Larkin sum rule relates the physical thermopower to the behaviours of all fractionalized components. The thermopower of neutral fermions, defined in relation to the emergent electric field, may be sensitive to the Landau quantization of the fermions[128,129]. An exact formulation for such a spin-charge separated insulator with Landau

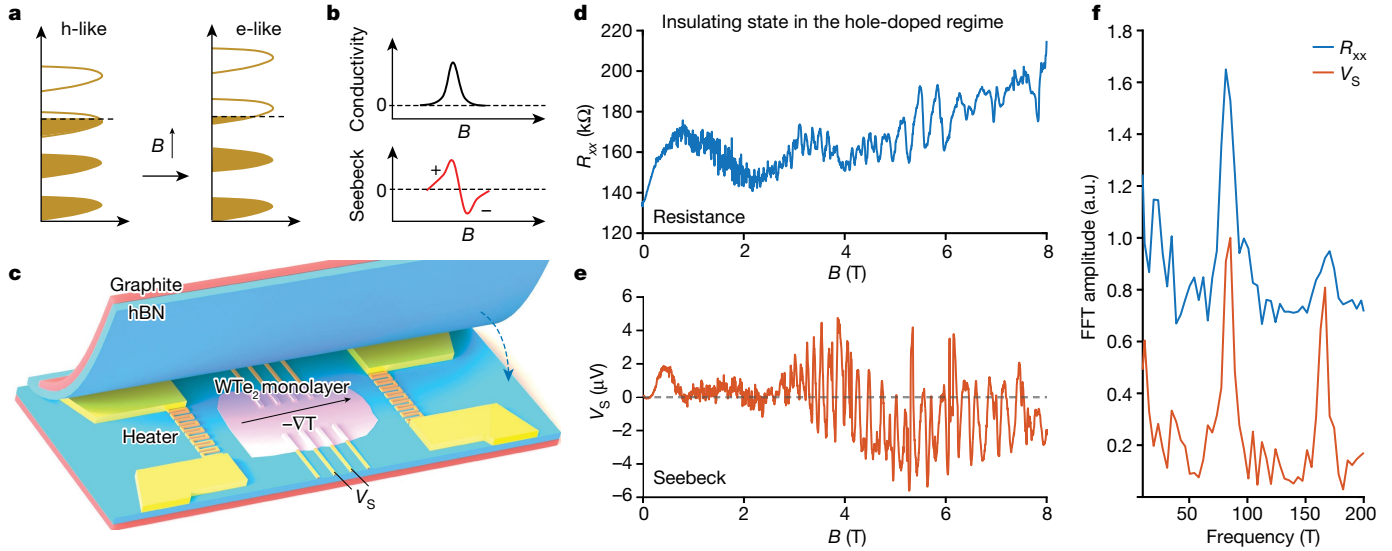

Fig. 4 | Transport and thermoelectric quantum oscillations in WTe_2 monolayer insulators. a, Illustration of Landau quantization in 2D electron gas. **b**, The response of conductivity and the Seebeck voltage signal when a Landau level passes the Fermi level induced by increasing magnetic fields. **c**, A cartoon illustration of a monolayer WTe_2 device for measuring both the transport and thermoelectricity in one device. **d**, Magnetoresistance of monolayer WTe_2 in the hole-doped insulating state, showing quantum oscillations. **e**, The Seebeck effect of the monolayer taken under the same condition, showing sign-change quantum oscillations. Data replotted from ref. 150. **f**, Fast Fourier transformation (FFT) of the oscillations, showing the same periods observed in resistance and the Seebeck effect. More discussions can be found in ref. 74.

quantization remains to be developed. The results identify 2D WTe_2 as an intriguing platform for investigating unconventional insulators.

More experimental probes are desirable to extend investigation of the quantum oscillations in 2D and 3D quantum insulators. The efforts towards confirming the true nature of insulating WTe_2 and its puzzling Landan quantization problem will lead to the development of a new set of tools for diagnosing 2D insulators. It is exciting that we now have several concrete 2D material platforms, including WTe_2, 1T-TaS_2/1T-$TaSe_2$ and α-$RuCl_3$, to explore the possibilities of neutral fermions, charge-neutral Fermi surface and other neutral phases in insulators. More candidate materials will surely emerge in the future.

Quest for new materials, experiments and theories

What is necessary to advance the research includes the developments of new quantum insulators, new detection schemes, innovative device structures and a new theoretical understanding of next-generation quantum effects in insulators. Such endeavours require synergetic efforts between chemists, experimentalists and theorists.

New materials

New synthesis of quantum materials in both the bulk and 2D forms is crucial. Recent examples of new Kitaev materials include Ru-based[153] (for example, RuI_3) and Co-based[154–156] honeycomb lattice materials (for example, $BaCo_2(AsO_4)_2$). 2D forms of quantum insulators are still rarely explored and hold great promise, yet we already have several target materials including but not limited to the several cases that we highlighted in this article. The unique advantages of gate turnabilities and interface effects, especially by means of moiré quantum engineering, in 2D vdW crystals may provide entirely new possibilities in addressing some key issues. For instance, beyond monolayers, twisted bilayers of QSL may allow for quantum engineering of spinon bands.

New detection schemes

The detection of neutral excitations in condensed matter requires innovative techniques beyond conventional means. For instance, although we have no issues with fabricating high-quality devices of monolayer and twisted bilayer 1T-TaS_2, we do not have an approach to uncover its electronic properties at low T. Recently, far-infrared optical spectroscopy of quantum materials at millikelvin temperatures and in magnetic fields has been developed[157], which might be helpful moving forward. Optical means can in principle access neutral excitations that are not visible in charge transport. For example, optical resonances of ground state excitons may provide an unambiguous demonstration of excitonic insulators and distinguish their species. Fingerprints of a charge-neutral Fermi surface may be found in subgap optical resonances[29,32,76,158]. Similarly, probing techniques in the THz to GHz regime will probably be powerful, yet their applications in correlated quantum insulators, especially at ultralow T and in strong B, remain largely unexplored. A promising avenue is to extract information of hidden excitations by 2D coherent spectroscopy[159–161]. Another exciting direction to explore is to use recent advances in quantum sensing for probing quantum matter. A proposal is to use nitrogen vacancy-centre spin qubits for detecting quantum noises of spinon Fermi surfaces[33,162–164].

Charge-neutral quantum devices

The investigations of neutral quantum phases in insulator will probably benefit the development of future quantum devices. The exploration of such devices will in turn further promote the study of quantum insulators. For instance, neutral excitonic or spinon phases may allow for low-power consumption transistors without suffering Joule heating (as it does not involve charge transport). Simultaneously, chip-scale generation, non-local transport[165] and detection of neutral excitations could provide unique ways of proving the existence of hidden neutral modes. Such explorations will be essential in establishing the unique non-local properties of many neutral excitations of interest. A highly relevant topic is that the realization of electron fractionalization and anyons in insulators can in principle enable robust quantum computation schemes with topological protection[14].

New theoretical understanding

Despite the significant progress in theoretical understanding of a large class of non-trivial quantum insulators we still face serious challenges in bridging the divide between ideal theories, models, and materials.

One strategy for closing this divide is to search for new general principles that could enrich our search for the emergence of fractionalization in models and materials. For example, non-trivial band topology prevents the existence of a trivial localized flat-band Hubbard limit, because of the obstruction to constructing Wannier orbitals. This offers an enhancement of the quantum fluctuations induced by interactions that could favour non-trivial quantum orders in partially filled topological bands. In fact, this feature is intimately linked to why fractionalized phases are abundant in the limit of Landau levels, which are essentially ideal flat Chern bands. Although the link of non-trivial band topology to enhanced quantum fluctuations has been recently emphasized and investigated in moiré materials, understanding its broader implications and incarnations, for example in 3D materials, remains largely open. With the increasing numbers of 2D and 3D insulators with non-trivial topological band structures, the need to better understand the interplay of band topology and strong interactions is pressing.

Another important challenge is to develop the theory of new experimental probes that help identify and characterize the presence of non-trivial states in materials. For example, nitrogen vacancy-centre noise spectroscopy is a promising tool that could help overcome some of the difficulties of nuclear magnetic resonance in 2D settings, and could help identify different non-trivial states[33,162–164]. More generally there is a need to develop our understanding of probes that could guide better the detection and characterization of non-trivial states in correlated materials.

Summary and outlook

In this Perspective, we have provided our views on a class of intriguing problems of quantum insulators and reviewed their status in theory and experiment. The topics discussed are selected to emphasize what we believe are the major challenges and promises in the field. Space restrictions prevent inclusion of many other recent findings. An example is the fractional quantum anomalous Hall effect[166–171] in fractional Chern insulators[172–176] recently observed in moiré materials. The rapid pace of discovery suggests that research in charge-neutral phases, excitations and phase transitions in fractionalized moiré materials will be an exciting area in the next few years.

The challenges in detecting hidden phenomena in insulators seem to recall how electromagnetic waves were first detected. We have made analogies between neutral fermions coupled to the emergent gauge field and electrons coupled to electromagnetic fields. The Hertz experiments[177], performed two decades after publication of Maxwell's equations, transformed the communication industry. Success in detecting neutral excitations and emergent gauge fields in quantum insulators may have a similar impact.

1. Giamarchi, T. *Quantum Physics in One Dimension* (Oxford Univ. Press, 2003).
2. Lee, P. A., Nagaosa, N. & Wen, X.-G. Doping a Mott insulator: physics of high-temperature superconductivity. *Rev. Mod. Phys.* **78**, 17–85 (2006).
3. Coleman, P. Theories of non-Fermi liquid behavior in heavy fermions. *Phys. B Condens. Matter* **259–261**, 353–358 (1999).
4. Stewart, G. R. Non-Fermi-liquid behavior in *d*- and *f*-electron metals. *Rev. Mod. Phys.* **73**, 797–855 (2001).
5. Cao, Y. et al. Strange metal in magic-angle graphene with near Planckian dissipation. *Phys. Rev. Lett.* **124**, 076801 (2020).
6. Jaoui, A. et al. Quantum critical behaviour in magic-angle twisted bilayer graphene. *Nat. Phys.* **18**, 633–638 (2022).
7. Wang, P. et al. One-dimensional Luttinger liquids in a two-dimensional moiré lattice. *Nature* **605**, 57–62 (2022).
8. Yu, G. et al. Evidence for two dimensional anisotropic Luttinger liquids at Millikelvin temperatures. *Nat. Commun.* **14**, 7025 (2023).
9. Jackiw, R. & Rebbi, C. Solitons with fermion number ½. *Phys. Rev. D* **13**, 3398–3409 (1976).
10. Su, W. P., Schrieffer, J. R. & Heeger, A. J. Solitons in polyacetylene. *Phys. Rev. Lett.* **42**, 1698–1701 (1979).
11. Tsui, D. C., Stormer, H. L. & Gossard, A. C. Two-dimensional magnetotransport in the extreme quantum limit. *Phys. Rev. Lett.* **48**, 1559–1562 (1982).
12. Arovas, D., Schrieffer, J. R. & Wilczek, F. Fractional statistics and the quantum Hall effect. *Phys. Rev. Lett.* **53**, 722–723 (1984).
13. Stern, A. Anyons and the quantum Hall effect—a pedagogical review. *Ann. Phys.* **323**, 204–249 (2008).
14. Nayak, C., Simon, S. H., Stern, A., Freedman, M. & Das Sarma, S. Non-Abelian anyons and topological quantum computation. *Rev. Mod. Phys.* **80**, 1083–1159 (2008).
15. Anderson, P. W. Resonating valence bonds: a new kind of insulator? *Mater. Res. Bull.* **8**, 153–160 (1973).
This paper proposed the RVB state, which initiated the research of spin liquids.
16. Anderson, P. W. The resonating valence bond state in La_2CuO_4 and superconductivity. *Science* **235**, 1196–1198 (1987).
17. Moessner, R. & Sondhi, S. L. Resonating valence bond phase in the triangular lattice quantum dimer model. *Phys. Rev. Lett.* **86**, 1881–1884 (2001).
This paper concluded the search for an RVB liquid by demonstrating its existence in a microscopic model.
18. Moessner, R. & Moore, J. E. *Topological Phases of Matter* (Cambridge Univ. Press, 2021).
19. Kitaev, A. Y. Fault-tolerant quantum computation by anyons. *Ann. Phys.* **303**, 2–30 (2003).
20. Wen, X.-G. Quantum orders and symmetric spin liquids. *Phys. Rev. B* **65**, 165113 (2002).
21. Read, N. & Chakraborty, B. Statistics of the excitations of the resonating-valence-bond state. *Phys. Rev. B* **40**, 7133–7140 (1989).
22. Kalmeyer, V. & Laughlin, R. B. Equivalence of the resonating-valence-bond and fractional quantum Hall states. *Phys. Rev. Lett.* **59**, 2095–2098 (1987).
23. Pace, S. D., Morampudi, S. C., Moessner, R. & Laumann, C. R. Emergent fine structure constant of quantum spin ice is large. *Phys. Rev. Lett.* **127**, 117205 (2021).
24. Hermele, M. et al. Stability of U(1) spin liquids in two dimensions. *Phys. Rev. B* **70**, 214437 (2004).
25. Lee, S.-S. Stability of the U(1) spin liquid with a spinon Fermi surface in 2+1 dimensions. *Phys. Rev. B* **78**, 085129 (2008).
26. Huse, D. A., Krauth, W., Moessner, R. & Sondhi, S. L. Coulomb and liquid dimer models in three dimensions. *Phys. Rev. Lett.* **91**, 167004 (2003).
27. Hermele, M., Fisher, M. P. A. & Balents, L. Pyrochlore photons: the U(1) spin liquid in a *S*=1/2 three-dimensional frustrated magnet. *Phys. Rev. B* **69**, 064404 (2004).
28. Castelnovo, C., Moessner, R. & Sondhi, S. L. Magnetic monopoles in spin ice. *Nature* **451**, 42–45 (2008).
29. Ng, T.-K. & Lee, P. A. Power-law conductivity inside the Mott gap: application to κ-(BEDT–TTF)$_2$Cu$_2$(CN)$_3$. *Phys. Rev. Lett.* **99**, 156402 (2007).
30. Motrunich, O. I. Orbital magnetic field effects in spin liquid with spinon Fermi sea: possible application to κ-(ET)$_2$ (Cu)$_2$(CN)$_3$. *Phys. Rev. B* **73**, 155115 (2006).
This paper predicted spinon Landau quantization in magnetic fields, a key step in the search for neutral fermions using quantum oscillations.
31. Sodemann, I., Chowdhury, D. & Senthil, T. Quantum oscillations in insulators with neutral Fermi surfaces. *Phys. Rev. B* **97**, 045152 (2018).
This paper developed a theory of quantum oscillations in observables such as resistance and magnetization induced by spinon Landau quantization.
32. Rao, P. & Sodemann, I. Cyclotron resonance inside the Mott gap: a fingerprint of emergent neutral fermions. *Phys. Rev. B* **100**, 155150 (2019).
33. Khoo, J. Y., Pientka, F., Lee, P. A. & Villadiego, I. S. Probing the quantum noise of the spinon Fermi surface with NV centers. *Phys. Rev. B* **106**, 115108 (2022).
34. Jérome, D., Rice, T. M. & Kohn, W. Excitonic insulator. *Phys. Rev.* **158**, 462–475 (1967).
35. Kohn, W. Excitonic phases. *Phys. Rev. Lett.* **19**, 439–442 (1967).
36. Blatt, J. M., Böer, K. W. & Brandt, W. Bose-Einstein condensation of excitons. *Phys. Rev.* **126**, 1691–1692 (1962).
37. Mott, N. F. The transition to the metallic state. *Philos. Mag.* **6**, 287–309 (1961).
38. Halperin, B. I. & Rice, T. M. Possible anomalies at a semimetal-semiconductor transition. *Rev. Mod. Phys.* **40**, 755–766 (1968).
39. Kwan, Y. H., Devakul, T., Sondhi, S. L. & Parameswaran, S. A. Theory of competing excitonic orders in insulating WTe_2 monolayers. *Phys. Rev. B* **104**, 125133 (2021).
40. Wang, Y.-Q., Papaj, M. & Moore, J. E. Breakdown of helical edge state topologically protected conductance in time-reversal-breaking excitonic insulators. *Phys. Rev. B* **108**, 205420 (2023).
41. Hu, Y., Venderbos, J. W. F. & Kane, C. L. Fractional excitonic insulator. *Phys. Rev. Lett.* **121**, 126601 (2018).
42. Chowdhury, D., Sodemann, I. & Senthil, T. Mixed-valence insulators with neutral Fermi surfaces. *Nat. Commun.* **9**, 1766 (2018).
43. Xu, X., Yao, W., Xiao, D. & Heinz, T. F. Spin and pseudospins in layered transition metal dichalcogenides. *Nat. Phys.* **10**, 343–350 (2014).
44. Wang, G. et al. Colloquium: excitons in atomically thin transition metal dichalcogenides. *Rev. Mod. Phys.* **90**, 021001 (2018).
45. Eisenstein, J. P. Exciton condensation in bilayer quantum Hall systems. *Annu. Rev. Condens. Matter Phys.* **5**, 159–181 (2014).
46. Liu, X., Watanabe, K., Taniguchi, T., Halperin, B. I. & Kim, P. Quantum Hall drag of exciton condensate in graphene. *Nat. Phys.* **13**, 746–750 (2017).
47. Li, J. I. A., Taniguchi, T., Watanabe, K., Hone, J. & Dean, C. R. Excitonic superfluid phase in double bilayer graphene. *Nat. Phys.* **13**, 751–755 (2017).
48. Du, L. et al. Evidence for a topological excitonic insulator in InAs/GaSb bilayers. *Nat. Commun.* **8**, 1971 (2017).
49. Yu, W. et al. Anomalously large resistance at the charge neutrality point in a zero-gap InAs/GaSb bilayer. *New J. Phys.* **20**, 053062 (2018).
50. Chen, D. et al. Excitonic insulator in a heterojunction moiré superlattice. *Nat. Phys.* **18**, 1171–1176 (2022).
51. Zhang, Z. et al. Correlated interlayer exciton insulator in heterostructures of monolayer WSe_2 and moiré WS_2/WSe_2. *Nat. Phys.* **18**, 1214–1220 (2022).
52. Ma, L. et al. Strongly correlated excitonic insulator in atomic double layers. *Nature* **598**, 585–589 (2021).
53. Cercellier, H. et al. Evidence for an excitonic insulator phase in 1T $TiSe_2$. *Phys. Rev. Lett.* **99**, 146403 (2007).
54. Kogar, A. et al. Signatures of exciton condensation in a transition metal dichalcogenide. *Science* **358**, 1314–1317 (2017).
55. Campbell, D. J. et al. Intrinsic insulating ground state in transition metal dichalcogenide $TiSe_2$. *Phys. Rev. Mater.* **3**, 053402 (2019).

56. Li, Z. et al. Possible excitonic insulating phase in quantum-confined Sb nanoflakes. *Nano Lett.* **19**, 4960–4964 (2019).
57. Wakisaka, Y. et al. Excitonic insulator state in Ta_2NiSe_5 probed by photoemission spectroscopy. *Phys. Rev. Lett.* **103**, 026402 (2009).
58. Lu, Y. F. et al. Zero-gap semiconductor to excitonic insulator transition in Ta_2NiSe_5. *Nat. Commun.* **8**, 14408 (2017).
59. Fukutani, K. et al. Electrical tuning of the excitonic insulator ground state of Ta_2NiSe_5. *Phys. Rev. Lett.* **123**, 206401 (2019).
60. Werdehausen, D. et al. Coherent order parameter oscillations in the ground state of the excitonic insulator Ta_2NiSe_5. *Sci. Adv.* **4**, eaap8652 (2018).
61. Baldini, E. et al. The spontaneous symmetry breaking in Ta_2NiSe_5 is structural in nature. *Proc. Natl Acad. Sci. USA* **120**, e2221688120 (2023).
62. Hossain, M. S. et al. Discovery of a topological exciton insulator with tunable momentum order. Preprint at https://arxiv.org/abs/2312.15862 (2023).
63. Huang, J. et al. Evidence for an excitonic insulator state in $Ta_2Pd_3Te_5$. *Phys. Rev. X* **14**, 011046 (2024).
64. Jia, Y. et al. Evidence for a monolayer excitonic insulator. *Nat. Phys.* **18**, 87–93 (2022).
This paper, together with ref. 65, identified a 2D natural crystal (monolayer WTe_2) as an excitonic insulator.
65. Sun, B. et al. Evidence for equilibrium exciton condensation in monolayer WTe_2. *Nat. Phys.* **18**, 94–99 (2022).
This paper, together with ref. 64, identified a 2D natural crystal (monolayer WTe_2) as an excitonic insulator.
66. Lee, P. A. Quantum oscillations in the activated conductivity in excitonic insulators: possible application to monolayer WTe_2. *Phys. Rev. B* **103**, L041101 (2021).
67. Qian, X., Liu, J., Fu, L. & Li, J. Quantum spin Hall effect in two-dimensional transition metal dichalcogenides. *Science* **346**, 1344–1347 (2014).
68. Fei, Z. et al. Edge conduction in monolayer WTe_2. *Nat. Phys.* **13**, 677–682 (2017).
69. Tang, S. et al. Quantum spin Hall state in monolayer 1T′-WTe_2. *Nat. Phys.* https://doi.org/10.1038/nphys4174 (2017).
70. Wu, S. et al. Observation of the quantum spin Hall effect up to 100 kelvin in a monolayer crystal. *Science* **359**, 76–79 (2018).
71. Fatemi, V. et al. Electrically tunable low-density superconductivity in a monolayer topological insulator. *Science* **362**, 926–929 (2018).
72. Sajadi, E. et al. Gate-induced superconductivity in a monolayer topological insulator. *Science* **362**, 922–925 (2018).
73. Wang, P. et al. Landau quantization and highly mobile fermions in an insulator. *Nature* **589**, 225–229 (2021).
This paper, together with ref. 74, reported quantum oscillations in monolayer WTe_2 insulator.
74. Tang, Y. et al. Sign-alternating thermoelectric quantum oscillations and insulating Landau levels in monolayer WTe_2. Preprint at https://arxiv.org/abs/2405.09665 (2024).
This paper, together with ref. 73, reported quantum oscillations in monolayer WTe_2 insulator.
75. Song, T. et al. Unconventional superconducting quantum criticality in monolayer WTe_2. *Nat. Phys.* **20**, 269–274 (2024).
76. He, W.-Y. & Lee, P. A. Electronic density of states of a U(1) quantum spin liquid with spinon Fermi surface. I. Orbital magnetic field effects. *Phys. Rev. B* **107**, 195155 (2023).
77. Zhou, Y., Kanoda, K. & Ng, T.-K. Quantum spin liquid states. *Rev. Mod. Phys.* **89**, 025003 (2017).
78. Broholm, C. et al. Quantum spin liquids. *Science* **367**, eaay0668 (2020).
79. Knolle, J. & Moessner, R. A field guide to spin liquids. *Annu. Rev. Condens. Matter Phys.* **10**, 451–472 (2019).
80. Takagi, H., Takayama, T., Jackeli, G., Khaliullin, G. & Nagler, S. E. Concept and realization of Kitaev quantum spin liquids. *Nat. Rev. Phys.* **1**, 264–280 (2019).
81. Savary, L. & Balents, L. Quantum spin liquids: a review. *Rep. Prog. Phys.* **80**, 016502 (2017).
82. Law, K. T. & Lee, P. A. 1T-TaS_2 as a quantum spin liquid. *Proc. Natl Acad. Sci. USA* **114**, 6996–7000 (2017).
83. He, W.-Y., Xu, X. Y., Chen, G., Law, K. T. & Lee, P. A. Spinon Fermi surface in a cluster Mott insulator model on a triangular lattice and possible application to 1T-TaS_2. *Phys. Rev. Lett.* **121**, 046401 (2018).
84. Sipos, B. et al. From Mott state to superconductivity in 1T-TaS_2. *Nat. Mater.* **7**, 960–965 (2008).
85. Yu, Y. et al. Gate-tunable phase transitions in thin flakes of 1T-TaS_2. *Nat. Nanotechnol.* **10**, 270–276 (2015).
86. Wang, Y. D. et al. Band insulator to Mott insulator transition in 1T-TaS_2. *Nat. Commun.* **11**, 4215 (2020).
87. Ritschel, T., Berger, H. & Geck, J. Stacking-driven gap formation in layered 1T-TaS_2. *Phys. Rev. B* **98**, 195134 (2018).
88. Wu, Z. et al. Effect of stacking order on the electronic state of 1T-TaS_2. *Phys. Rev. B* **105**, 035109 (2022).
89. Chen, Y. et al. Strong correlations and orbital texture in single-layer 1T-$TaSe_2$. *Nat. Phys.* **16**, 218–224 (2020).
90. Ruan, W. et al. Evidence for quantum spin liquid behaviour in single-layer 1T-$TaSe_2$ from scanning tunnelling microscopy. *Nat. Phys.* **17**, 1154–1161 (2021).
91. Chen, Y. et al. Evidence for a spinon Kondo effect in cobalt atoms on single-layer 1T-$TaSe_2$. *Nat. Phys.* **18**, 1335–1340 (2022).
92. Zhang, Q. et al. Quantum spin liquid signatures in monolayer 1T-$NbSe_2$. *Nat. Commun.* **15**, 2336 (2024).
93. Liu, L. et al. Direct identification of Mott Hubbard band pattern beyond charge density wave superlattice in monolayer 1T-$NbSe_2$. *Nat. Commun.* **12**, 1978 (2021).
94. Liu, M. et al. Monolayer 1T-$NbSe_2$ as a 2D-correlated magnetic insulator. *Sci. Adv.* **7**, eabi6339 (2021).
95. Nakata, Y. et al. Monolayer 1T-$NbSe_2$ as a Mott insulator. *NPG Asia Mater.* **8**, e321–e321 (2016).
96. Kitaev, A. Anyons in an exactly solved model and beyond. *Ann. Phys.* **321**, 2–111 (2006).
This paper provided an exactly solvable model for quantum spin liquids.
97. Jackeli, G. & Khaliullin, G. Mott insulators in the strong spin-orbit coupling limit: from Heisenberg to a quantum compass and Kitaev models. *Phys. Rev. Lett.* **102**, 017205 (2009).
98. Banerjee, A. et al. Proximate Kitaev quantum spin liquid behaviour in a honeycomb magnet. *Nat. Mater.* **15**, 733–740 (2016).
99. Plumb, K. W. et al. α-$RuCl_3$: a spin-orbit assisted Mott insulator on a honeycomb lattice. *Phys. Rev. B* **90**, 041112 (2014).
100. Leahy, I. A. et al. Anomalous thermal conductivity and magnetic torque response in the honeycomb magnet α-$RuCl_3$. *Phys. Rev. Lett.* **118**, 187203 (2017).
101. Banerjee, A. et al. Excitations in the field-induced quantum spin liquid state of α-$RuCl_3$. *npj Quantum Mater.* **3**, 8 (2018).
102. Hentrich, R. et al. Unusual phonon heat transport in α-$RuCl_3$: strong spin-phonon scattering and field-induced spin gap. *Phys. Rev. Lett.* **120**, 117204 (2018).
103. McClarty, P. A. et al. Topological magnons in Kitaev magnets at high fields. *Phys. Rev. B* **98**, 060404 (2018).
104. Joshi, D. G. Topological excitations in the ferromagnetic Kitaev-Heisenberg model. *Phys. Rev. B* **98**, 060405 (2018).
105. Gordon, J. S., Catuneanu, A., Sørensen, E. S. & Kee, H.-Y. Theory of the field-revealed Kitaev spin liquid. *Nat. Commun.* **10**, 2470 (2019).
106. Hickey, C. & Trebst, S. Emergence of a field-driven U(1) spin liquid in the Kitaev honeycomb model. *Nat. Commun.* **10**, 530 (2019).
107. Ponomaryov, A. N. et al. Nature of magnetic excitations in the high-field phase of α-$RuCl_3$. *Phys. Rev. Lett.* **125**, 037202 (2020).
108. Wang, Z. et al. Magnetic excitations and continuum of a possibly field-induced quantum spin liquid in α-$RuCl_3$. *Phys. Rev. Lett.* **119**, 227202 (2017).
109. Czajka, P. et al. Planar thermal Hall effect of topological bosons in the Kitaev magnet α-$RuCl_3$. *Nat. Mater.* **22**, 36–41 (2023).
This paper reported the thermal Hall data incompatible with the half-quantization expected for the Majorana transport in α-$RuCl_3$.
110. Czajka, P. et al. Oscillations of the thermal conductivity in the spin-liquid state of α-$RuCl_3$. *Nat. Phys.* **17**, 915–919 (2021).
This paper reported the magneto-oscillations in the thermal conductivity of α-$RuCl_3$.
111. Kasahara, Y. et al. Majorana quantization and half-integer thermal quantum Hall effect in a Kitaev spin liquid. *Nature* **559**, 227–231 (2018).
112. Yokoi, T. et al. Half-integer quantized anomalous thermal Hall effect in the Kitaev material candidate α-$RuCl_3$. *Science* **373**, 568–572 (2021).
113. Zhang, E. Z., Chern, L. E. & Kim, Y. B. Topological magnons for thermal Hall transport in frustrated magnets with bond-dependent interactions. *Phys. Rev. B* **103**, 174402 (2021).
114. Bruin, J. A. N. et al. Robustness of the thermal Hall effect close to half-quantization in α-$RuCl_3$. *Nat. Phys.* **18**, 401–405 (2022).
115. Villadiego, I. S. Pseudoscalar U(1) spin liquids in α-$RuCl_3$. *Phys. Rev. B* **104**, 195149 (2021).
116. Bruin, J. A. N. et al. Origin of oscillatory structures in the magnetothermal conductivity of the putative Kitaev magnet α-$RuCl_3$. *APL Mater.* **10**, 090703 (2022).
117. Kubota, Y., Tanaka, H., Ono, T., Narumi, Y. & Kindo, K. Successive magnetic phase transitions in α-$RuCl_3$: *XY*-like frustrated magnet on the honeycomb lattice. *Phys. Rev. B* **91**, 094422 (2015).
118. Cao, H. B. et al. Low-temperature crystal and magnetic structure of α-$RuCl_3$. *Phys. Rev. B* **93**, 134423 (2016).
119. Lefrançois, É. et al. Oscillations in the magnetothermal conductivity of α–$RuCl_3$: evidence of transition anomalies. *Phys. Rev. B* **107**, 064408 (2023).
120. Zhang, H. et al. Sample-dependent and sample-independent thermal transport properties of α-$RuCl_3$. *Phys. Rev. Mater.* **7**, 114403 (2023).
121. Zhang, H. et al. Stacking disorder and thermal transport properties of α-$RuCl_3$. *Phys. Rev. Mater.* **8**, 014402 (2024).
122. Zhang, H. et al. Anisotropy of thermal conductivity oscillations in relation to the Kitaev spin liquid phase. Preprint at https://arxiv.org/abs/2310.03917 (2023).
123. Hong, X. et al. Phonon thermal transport shaped by strong spin-phonon scattering in a Kitaev material $Na_2Co_2TeO_6$. *npj Quantum Mater.* **9**, 18 (2024).
124. Hong, X. et al. Spinon heat transport in the three-dimensional quantum magnet $PbCuTe_2O_6$. *Phys. Rev. Lett.* **131**, 256701 (2023).
125. Yamashita, M. et al. Presence and absence of itinerant gapless excitations in the quantum spin liquid candidate $EtMe_2Sb[Pd(dmit)_2]_2$. *Phys. Rev. B* **101**, 140407 (2020).
126. Ni, J. M. et al. Absence of magnetic thermal conductivity in the quantum spin liquid candidate $EtNe_3Sb[Pd(dmit)_2]_2$. *Phys. Rev. Lett.* **123**, 247204 (2019).
127. Bourgeois-Hope, P. et al. Thermal conductivity of the quantum spin liquid candidate $EtMe_3Sb[Pd(dnit)_2]_2$: no evidence of mobile gapless excitations. *Phys. Rev. X* **9**, 041051 (2019).
128. Ioffe, L. B. & Larkin, A. I. Gapless fermions and gauge fields in dielectrics. *Phys. Rev. B* **39**, 8988–8999 (1989).
This paper developed the so-called Ioffe-Larkin rule, which is important for understanding response functions of fractionalized systems.
129. Lee, P. A. & Nagaosa, N. Gauge theory of the normal state of high-Tc superconductors. *Phys. Rev. B* **46**, 5621–5639 (1992).
130. He, W.-Y. & Lee, P. A. Electronic density of states of a U1 quantum spin liquid with spinon Fermi surface. I. Orbital magnetic field effects. *Phys. Rev. B* **107**, 195155 (2023).
131. Tan, B. S. et al. Unconventional Fermi surface in an insulating state. *Science* **349**, 287–290 (2015).
132. Li, G. et al. Two-dimensional Fermi surfaces in Kondo insulator SmB6. *Science* **346**, 1208–1212 (2014).
133. Xiang, Z. et al. Quantum oscillations of electrical resistivity in an insulator. *Science* **362**, 65–69 (2018).
134. Han, Z., Li, T., Zhang, L., Sullivan, G. & Du, R.-R. Anomalous conductance oscillations in the hybridization gap of InAs/GaSb quantum wells. *Phys. Rev. Lett.* **123**, 126803 (2019).
135. Xiao, D., Liu, C.-X., Samarth, N. & Hu, L.-H. Anomalous quantum oscillations of interacting electron-hole gases in inverted type-II InAs/GaSb quantum wells. *Phys. Rev. Lett.* **122**, 186802 (2019).

136. Zheng, G. et al. Unconventional magnetic oscillations in Kagome Mott insulators. Preprint at *arXiv* https://arxiv.org/abs/2310.07989 (2023).
137. Li, L., Sun, K., Kurdak, C. & Allen, J. W. Emergent mystery in the Kondo insulator samarium hexaboride. *Nat. Rev. Phys.* **2**, 463–479 (2020).
138. Shen, H. & Fu, L. Quantum oscillation from in-gap states and a non-Hermitian Landau level problem. *Phys. Rev. Lett.* **121**, 026403 (2018).
139. Zhang, L., Song, X.-Y. & Wang, F. Quantum oscillation in narrow-gap topological insulators. *Phys. Rev. Lett.* **116**, 046404 (2016).
140. Ram, P. & Kumar, B. Theory of quantum oscillations of magnetization in Kondo insulators. *Phys. Rev. B* **96**, 075115 (2017).
141. Knolle, J. & Cooper, N. R. Quantum oscillations without a Fermi surface and the anomalous de Haas–van Alphen effect. *Phys. Rev. Lett.* **115**, 146401 (2015).
142. Knolle, J. & Cooper, N. R. Anomalous de Haas–van Alphen effect in InAs/GaSb quantum wells. *Phys. Rev. Lett.* **118**, 176801 (2017).
143. Erten, O., Chang, P.-Y., Coleman, P. & Tsvelik, A. M. Skyrme insulators: insulators at the brink of superconductivity. *Phys. Rev. Lett.* **119**, 057603 (2017).
144. He, W.-Y. & Lee, P. A. Quantum oscillation of thermally activated conductivity in a monolayer WTe2-like excitonic insulator. *Phys. Rev. B* **104**, L041110 (2021).
145. Zhu, J., Li, T., Young, A. F., Shan, J. & Mak, K. F. Quantum oscillations in 2D insulators induced by graphite gates. *Phys. Rev. Lett.* **127**, 247702 (2021).
146. Cooper, N. R. & Kelsall, J. Quantum oscillations in an impurity-band Anderson insulator. *Sci. Post Phys.***15**, 118 (2023).
147. Pirie, H. et al. Visualizing the atomic-scale origin of metallic behavior in Kondo insulators. *Science* **379**, 1214–1218 (2023).
148. Pal, H. K., Piéchon, F., Fuchs, J.-N., Goerbig, M. & Montambaux, G. Chemical potential asymmetry and quantum oscillations in insulators. *Phys. Rev. B* **94**, 125140 (2016).
149. Singh, G. & Pal, H. K. Effect of many-body interaction on de Haas–van Alphen oscillations in insulators. *Phys. Rev. B* **108**, L201103 (2023).
150. Wu, S. The detection of unconventional quantum oscillations in insulating 2D materials. *2D Mater.* **11**, 033004 (2024).
151. Checkelsky, J. G. & Ong, N. P. Thermopower and Nernst effect in graphene in a magnetic field. *Phys. Rev. B* **80**, 81413 (2009).
152. Zuev, Y. M., Chang, W. & Kim, P. Thermoelectric and magnetothermoelectric transport measurements of graphene. *Phys. Rev. Lett.* **102**, 96807 (2009).
153. Ni, D., Gui, X., Powderly, K. M. & Cava, R. J. Honeycomb-structure RuI_3, a new quantum material related to α-$RuCl_3$. *Adv. Mater.* **34**, e2106831 (2022).
154. Zhong, R., Gao, T., Ong, N. P. & Cava, R. J. Weak-field induced nonmagnetic state in a Co-based honeycomb. *Sci. Adv.* **6**, eaay6953 (2020).
155. Zhang, X. et al. A magnetic continuum in the cobalt-based honeycomb magnet $BaCo_2(AsO_4)_2$. *Nat. Mater.* **22**, 58–63 (2023).
156. Halloran, T. et al. Geometrical frustration versus Kitaev interactions in $BaCo_2(AsO_4)_2$. *Proc. Natl Acad. Sci. USA* **120**, e2215509119 (2023).
157. Onyszczak, M. et al. A platform for far-infrared spectroscopy of quantum materials at millikelvin temperatures. *Rev. Sci. Instrum.* **94**, 103903 (2023).
158. Potter, A. C., Senthil, T. & Lee, P. A. Mechanisms for sub-gap optical conductivity in Herbertsmithite. *Phys. Rev. B* **87**, 245106 (2013).
159. Wan, Y. & Armitage, N. P. Resolving continua of fractional excitations by spinon echo in THz 2D coherent spectroscopy. *Phys. Rev. Lett.* **122**, 257401 (2019).
160. Hart, O. & Nandkishore, R. Extracting spinon self-energies from two-dimensional coherent spectroscopy. *Phys. Rev. B* **107**, 205143 (2023).
161. Gao, Q., Liu, Y., Liao, H. & Wan, Y. Two-dimensional coherent spectrum of interacting spinons from matrix product states. *Phys. Rev. B* **107**, 165121 (2023).
162. Chatterjee, S., Rodriguez-Nieva, J. F. & Demler, E. Diagnosing phases of magnetic insulators via noise magnetometry with spin qubits. *Phys. Rev. B* **99**, 104425 (2019).
163. Khoo, J. Y., Pientka, F. & Sodemann, I. The universal shear conductivity of Fermi liquids and spinon Fermi surface states and its detection via spin qubit noise magnetometry. *New J. Phys.* **23**, 113009 (2021).
164. Lee, P. A. & Morampudi, S. Proposal to detect emergent gauge field and its Meissner effect in spin liquids using NV centers. *Phys. Rev. B* **107**, 195102 (2023).
165. Han, W., Maekawa, S. & Xie, X.-C. Spin current as a probe of quantum materials. *Nat. Mater.* **19**, 139–152 (2020).
166. Park, H. et al. Observation of fractionally quantized anomalous Hall effect. *Nature* **622**, 74–79 (2023).
This paper reported the fractional quantum anomalous Hall effect.
167. Xu, F. et al. Observation of integer and fractional quantum anomalous Hall effects in twisted bilayer $MoTe_2$. *Phys. Rev. X* **13**, 031037 (2023).
168. Lu, Z. et al. Fractional quantum anomalous Hall effect in multilayer graphene. *Nature* **626**, 759–764 (2024).
169. Anderson, E. et al. Programming correlated magnetic states with gate-controlled moiré geometry. *Science* **381**, 325–330 (2023).
170. Cai, J. et al. Signatures of fractional quantum anomalous Hall states in twisted $MoTe_2$. *Nature* **622**, 63–68 (2023).
171. Zeng, Y. et al. Thermodynamic evidence of fractional Chern insulator in moiré $MoTe_2$. *Nature* **622**, 69–73 (2023).
172. Neupert, T., Santos, L., Chamon, C. & Mudry, C. Fractional quantum Hall states at zero magnetic field. *Phys. Rev. Lett.* **106**, 236804 (2011).
173. Sheng, D. N., Gu, Z.-C., Sun, K. & Sheng, L. Fractional quantum Hall effect in the absence of Landau levels. *Nat. Commun.* **2**, 389 (2011).
174. Regnault, N. & Bernevig, B. A. Fractional Chern insulator. *Phys. Rev. X* **1**, 021014 (2011).
175. Tang, E., Mei, J.-W. & Wen, X.-G. High-temperature fractional quantum Hall states. *Phys. Rev. Lett.* **106**, 236802 (2011).
176. Sun, K., Gu, Z., Katsura, H. & Das Sarma, S. Nearly flatbands with nontrivial topology. *Phys. Rev. Lett.* **106**, 236803 (2011).
177. Baird, D., Hughes, R. I. G. & Nordmann, A. *Heinrich Hertz: Classical Physicist, Modern Philosopher* (Springer-Verlag, 1998).
178. Laumann, C. R. & Moessner, R. Hybrid dyons, inverted Lorentz force, and magnetic Nernst effect in quantum spin ice. *Phys. Rev. B* **108**, L220402 (2023).
This paper predicted a novel variant of the Nernst effect in insulators induced by physics of quantum spin ice.

Acknowledgements S.W. acknowledges support from Gordon and Betty Moore Foundation's EPiQS Initiative grant no. GBMF11946, AFOSR through a Young Investigator Award (grant no. FA9550-23-1-0140), ONR through a Young Investigator Award (grant no. N00014-21-1-2804), NSF through a CAREER award (grant no. DMR-1942942) and the Sloan Foundation. N.P.O., R.J.C., L.M.S. and S.W. acknowledge support from the Materials Research Science and Engineering Center programme of the NSF (grant no. DMR-2011750). N.P.O. acknowledges support from the United States Department of Energy (grant no. DE-SC0017863) (which supported the κ_{xy} experiments on α-$RuCl_3$) and the Gordon and Betty Moore Foundation through grant no. GBMF9466. L.M.S. acknowledges support from the Gordon and Betty Moore Foundation through grant no. GBMF9064 and the David and Lucile Packard Foundation. S.W. and L.M.S. acknowledge support from the Eric and Wendy Schmidt Transformative Technology Fund at Princeton. The research on forefront electronic materials in the laboratory of R.J.C. at Princeton is supported by the Gordon and Betty Moore Foundation through grant GBMF-9066 and the US DOE division of Basic Energy Sciences (grant no. DE-FG02-98R45706). I.S. acknowledges support from the Deutsche Forschungsgemeinschaft through research grant project numbers 542614019 and 518372354. R.M. acknowledges funding by the Deutsche Forschungsgemeinschaft under grants SFB 1143 (project-id 247310070) and the cluster of excellence ct.qmat (grant no. EXC 2147, project-id 390858490).

Author contributions S.W. and N.P.O. initiated the work. I.S. and R.M. wrote the theory parts. S.W., N.P.O., R.J.C. and L.M.S. wrote the experimental parts. All authors discussed and contributed to the overall writing and revisions of this work.

Competing interests The authors declare no competing interests.

Additional information
Correspondence and requests for materials should be addressed to Sanfeng Wu or N. P. Ong.
Peer review information *Nature* thanks the anonymous reviewers for their contribution to the peer review of this work.
Reprints and permissions information is available at http://www.nature.com/reprints.

Publisher's note Springer Nature remains neutral with regard to jurisdictional claims in published maps and institutional affiliations.